Sulfur loss of ZnS nanomaterials synthesized by arc discharge

XUFENG WU*, TONG WANG
School of Electronic Science & Engineering, Southeast University, Nanjing, 210096, P. R. China

ZnS nanomaterials are synthesized by arc discharge with ZnS powder as raw materials. The sample is characterized by X-ray Diffraction, scanning electron microscopy, transmission electron microscopy. A lot of ZnS nanorods and nanoparticles are found in the sample. The ZnS nanorods with the diameters of 20- 40nm and the lengths of 100-250nm exhibit single crystals with hexagonal wurtzite structure, and the growth process of ZnS nanorods can be interpreted by the vapor-solid mechanism. Photoluminescence (PL) spectrum shows a blue emission at around 410nm and a green emission at around 520nm. A phenomenon of sulfur loss of ZnS nanostructures is observed which can be interpreted by the process of carbon thermal reduction and pyrolysis of ZnS. Sulfur loss can be resolved by adding abundant S in raw materials.

(Received September 4, 2012; accepted January 22, 2014)

Keywords: ZnS nanomaterials, Arc discharge, Sulfur loss, Photoluminescence

1. Introduction

The material, ZnS, is an important direct band-gap II-VI semiconductor with a wide band gap of 3.72 eV for the cubic phase [1] and 3.77eV for the hexagonal-wurtzite phase [2] at room temperature. Nanocrystalline ZnS attracted much attention because properties in nanoforms differ significantly from those in bulk crystal [3]. ZnS has potential applications in numerous areas like flat-panel displays [4], sensors [4], optoelectronics [5,6], photocatalysis [7], field-emission device [8], solar cells [9], etc. It is reported that UV lasing of ZnS nanowires [10] and nanoribbon [11] working at room temperature with a low threshold would be quite potentially feasible.

So far, various ZnS nanostructures including nanorods, naowires, nanobelts, and nanotubes have been produced by different synthesis techniques, such as the solvothermal process [12], liquid crystal method [13], thermal evaporation [14], chemical vapor deposition [15], electrochemical method [16], and pulsed laser vaporization [17], etc. Arc discharge method is simple, cost-effective, rapid, and could easily be implemented and adapted for mass production. The morphology of nanostructured materials prepared by arc discharge can be tuned by varying the partial pressure, the arc discharge current, the process duration and other physical conditions that constitute the arc discharge process [18]. To date, arc discharge has mainly been applied to synthesize carbon nanotubes [19]. Few studies on the fabrication of non-carbon nanostructures via this method are reported [18,20- 22]. To our knowledge no study on preparation of ZnS nanomaterials by arc discharge has been reported. We have reported the successful synthesis of ZnO nanorods by arc discharge [23, 24]. In this paper, we synthesized ZnS nanostructures by electric arc discharge of ZnS powder in argon ambient. The microstructure, spectral property and the growth mechanism of ZnS nanostructures were discussed.

2. Experimental procedure

The arc was generated between two electrodes in a quartz chamber filled with argon. The anode was a Φ6mm graphite rod with a Φ4 mm hole pressed with pure ZnS powder, and the cathode was a round graphite piece with the diameter of 30 mm. The discharge conditions were optimized to avoid the production of carbon nanotubes. DC current of 60A at a voltage of 24V was applied between two electrodes under a pressure of 500 Torr of Ar. A constant distance of about 1mm between two electrodes was maintained by a step-motor to stabilize the electric arc. Typical discharge time was about 15 seconds. A layer of wool-like white products was formed on the inner walls of the chamber. The sample was collected on glass sheets.

The crystal structure of the as-prepared products was characterized by X-ray Diffraction (XRD)(XD-3 X-ray diffractometer) with Cu-Kα radiation under an accelerating voltage of 30kV. The morphology of the sample was examined by a Sirion field emission scanning electron microscopy (FE-SEM) and a JEM2000EX transmission electron microscopy (TEM). Photoluminescence (PL) characteristic of the product was measured at room temperature on a Jobin-Yvon LABRAMHR spectrometer excited by a He-Cd laser at 325nm.

3. Results and discussion

The FE-SEM morphology of ZnS nanomaterials is shown in Fig. 1. The image shows that many nanorods have grown. The diameter of the nanorods varies from 20nm to 40nm, and the length varies from 100nm to 250nm. The nanorods have uniform diameters along their lengths.

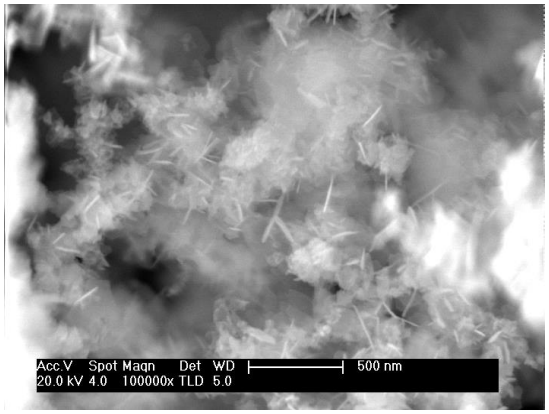

Fig. 1. SEM image of ZnS nanomaterials.

Fig. 2(a) indicates TEM image of single-crystalline ZnS nanorods. The diameter of the nanorods is about 30nm, and the length is about 100nm. And the corresponding selected area electron diffraction (SAED) pattern taken from the nanorod A in Fig. 2(a) is shown in Fig. 2(b). The results make it clear that the nanorod is single crystalline and grows alone [001] direction of ZnS which agree with the result of reference [25,26]. Otherwise, some nanoparticles locate at region B at the bottom of TEM image.

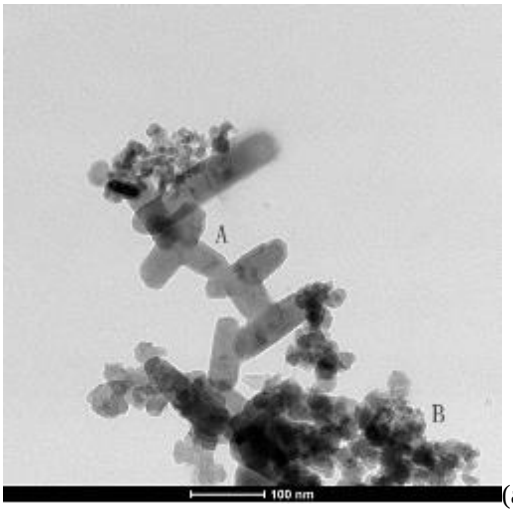

(a)

(b)

Fig. 2. (a) TEM image of ZnS nanomaterials (b) SAED pattern of nanorod A in Fig. 2(a).

Fig. 3 shows the XRD pattern of the ZnS products. The peaks can be indexed to be hexagonal wurtzite-structured ZnS with lattice parameters of a=0.3822nm and c=0.6260nm based on the hexagonal structure of bulk ZnS(JCPDS No. 792204). But a lot of metal Zn form based on the hexagonal structure of bulk Zn(JCPDS No. 040831).

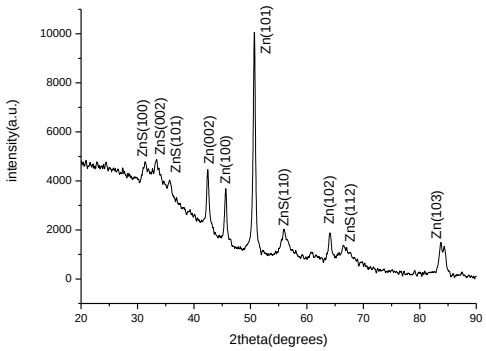

Fig. 3. XRD pattern of the ZnS nanomaterials.

The elements of products are analyzed by Energy dispersive of X-ray (EDX) attached on Sirion FE-SEM. The EDX spectrum shown in Fig. 4 reveals that the as-grown sample is composed of 64.59at.% Zn and 35.41at.% S. The result means that, during the course of arc discharge, some of sulfur is lost via carbon thermal reduction in the hole or pyrolysis of gaseous ZnS at high temperature, and a few elementary Zn form. Excess Zn form the under growth structures as shown in region B at the bottom of TEM image in Fig. 2(a). On the other hand, loss of sulfur will induce sulfur vacancies in ZnS crystal lattice.

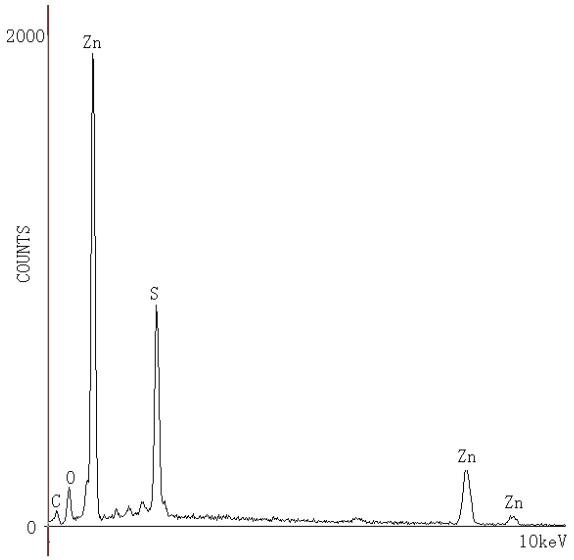

Fig. 4. The EDX spectrum of ZnS nanomaterials.

The method of arc discharge generates strongly nonequilibrium and inhomogenous temperature field. The arc can produce plasma with high temperature of more than 3000K caused by joule heating. The material is easy to be evaporated for Q-1D nanomaterials formation. But the method is restrained to fabricate non-carbon nanomaterials because of their poor electric conductivity. In our experiment, the raw material is filled in the hollow graphite rod as the anode. The electric and heat conductivity and the boiling point of the graphite are higher than those of the materials. So the temperature of materials rises quickly and the materials evaporate out fast. To minimize the ablation of carbon, the discharge current and time should be carefully controlled.

The melting point of ZnS is about 1700℃. At high temperature of more than 3000K produced by arc discharge ZnS decomposes into gaseous zinc and sulfur. The possible reaction is suggested in equation 1.

$$ZnS(l)\rightarrow Zn(g)+S(g) \quad (1)$$

Where (l) and (g) represent liquid and gas, respectively. The boiling point of sulfur (444.59℃) is lower than that of zinc(908℃). So sulfur is easy to be taken away by flowing argon. On the other hand, at lower temperature of about 600-800℃ hot carbon can reduce zinc from ZnS. The possible reaction is suggested in equation 2.

$$ZnS(s)+C\rightarrow Zn(l)+CS_2(g) \quad (2)$$

Where (s) represents solid. Gaseous CS_2 can be taken away by flowing argon and leads to sulfur loss. Because the reaction temperature of equation 2 is much lower than that of equation 1, the occurrence probability of equation 2 is larger than that of equation 1.

No metal top is found at the tip of ZnS nanorods in any SEM and TEM images. The result indicates that the growth of ZnS nanorods in our synthesis process may not be dominated by vapor-liquid-solid (VLS) mechanism in which a metal droplet is generally located at the growth front of the nanorods and acts as catalytic active site. So possible grown mechanism of ZnS nanorods is vapor-solid (VS) mechanism [27]. First, Zn atoms and S atoms produced via reactions of equation 1 and equation 2 combine to form ZnS nanoparticles with multiple-crystalline structure which are named the nuclear centers and unstable. In order to maintain the system in the lowest energy state, the terminal ZnS particles are formed and the growth on those ZnS particles starts. The Q-1D ZnS grows along one crystalline surface until it moves into the low temperature zone. During arc discharge, high temperature zone is very small and temperature gradient is very high to 10^3K/cm. So the diameter of ZnS nanrods is thin and the length is short. The ZnS particles in the zone of lower temperature cool down quickly which could not devote to growth of nanorods and form nanoparticles. The redundant Zn particles form nanoparticles too.

Fig. 5 shows the PL spectrum recorded at room temperature on a fluorescence spectrophotometer excited by a 325 nm light from He-Cd laser. The mean emitting bands, a blue emission at around 410nm, and a broad green emission at around 520nm are observed. The blue emission at 410 nm was reported to be the self-activated luminescence and ascribed to sulfur vacancies [28,29]. The green emission peak has been observed in co-doping ZnS by several groups [30]. But the as-synthesized ZnS nanomaterials is undoped according experimental procedure and EDX spectrum. Y. Jiang et al [31] infer that the green emission is caused by some self-activated center, probably vacancy states or interstitial states related to the peculiar nanostructure. We propose that the green emission centered at 520 nm may be related to structure defects such as point defects which could potentially induced deep-level emission. The small peak at 630 nm might be harmonic peak of 325 nm laser.

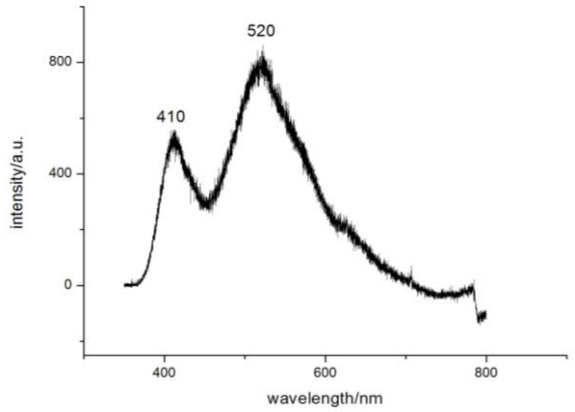

Fig. 5. Photoluminescence spectrum of ZnS nanomaterials at room temperature.

The experiment results mean that, during the growth of ZnS nanorods, some of sulfur loses in as-products via carbon thermal reduction or pyrolysis of ZnS. So another experiment is done using 50%at. ZnS +50%at. S as raw materials to compensate sulfur loss with abundant sulfur.

Fig. 6 shows the XRD pattern of the ZnS products with ZnS+S as raw materials. Only hexagonal wurtzite-structured ZnS (JCPDS No. 792204) and a little S (JCPDS No.861278) are found. While no metal Zn exists.

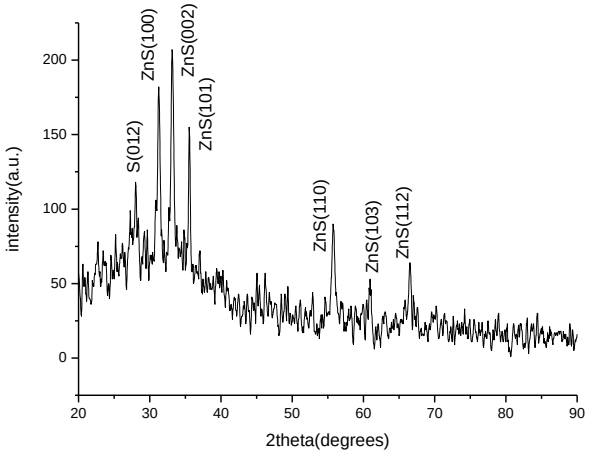

Fig. 6. XRD pattern of the ZnS nanomaterials with ZnS+S as raw materials.

TEM morphology of ZnS nanostructures with ZnS+S as raw materials shown in Fig. 7 is similar to that in Fig. 2. The diameters of ZnS nanorods are about 40nm, and the lengths are about 100-200nm. Some nanoparticles locate around ZnS nanorods. And EDX spectrum reveals that the as-grown sample has a composition of 49.16at.% Zn and 50.84at.% S. The results demonstrate that high-quality single-crystal ZnS nanorods are fabricated by arc discharge.

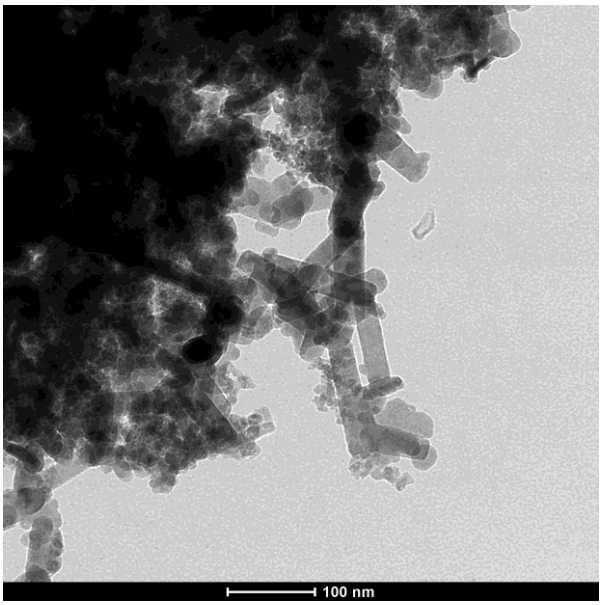

Fig. 7. TEM image of ZnS nanomaterials with ZnS+S as raw materials.

Fig. 8 shows the PL spectrum of ZnS nanorods using ZnS+S as raw materials excited by a 325 nm laser. Compare to Fig. 6, only the green emission at around 520nm is observed. The blue emission at around 410nm disappears. The result confirms that the blue emission at around 410nm of ZnS nanomaterials is ascribed to sulfur vacancies. The results also mean that sulfur loss is compensated by adding abundant sulfur in source materials.

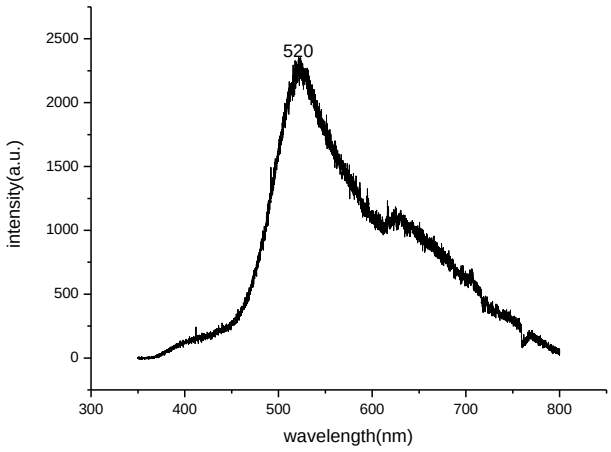

Fig. 8. PL spectrum of ZnS nanorods with ZnS+S as raw materials.

4. Conclusion

In Summary, we have fabricated ZnS nanostructures by the method of arc discharge. The sample is characterized by X-ray Diffraction, scanning electron

microscopy and transmission electron microscopy. Many ZnS nanorods and nanoparticles form. The ZnS nanorods exhibit hexagonal wurtzite structure. The diameters vary from 20nm to 40nm, and lengths vary from 100nm to 250nm. The growth process and the characteristics can be explained by VS mechanism. A blue emission at around 410nm and a green emission at around 520nm are observed in photoluminescence spectrum. A phenomenon of sulfur loss is observed in the experiment which can be explained by carbon thermal reduction or pyrolysis of ZnS, and can be resolved by adding abundant S in raw materials. This work provides a new method to produce Q-1D ZnS nanomaterials.

Acknowledgment

The work was supported by the National Natural Science Foundation of China (No.60977038).

References

[1] T. K. Tran, W. Park, W. Tong, M. M. Kyi, B. K. Wangner, C. J. Summers, J Appl Phys. **81**, 2803-9 (1997).
[2] H. C. Ong, R. P. Hchang, Appl Phys Lett. **79**, 3612-4 (2001).
[3] N. A. Dhas, A. Zaban, A. Gedanken, Characterization, and Optical Properties. Chem Mater. **11**, 806 (1999).
[4] H. J. Zhang, L. M. Qi, Nanotechnology, **17**, 3984-8 (2006).
[5] Y. W. Zhao, Y. Zhang, H. Zhu, G. C. Hadjipanayis, J. Q. Xiao, J Am Chem Soc; **126**, 6874-5 (2004).
[6] W. T. Yao, S. H. Yu, Q. S. Wu, Adv Funct Mater; **17**, 623-31 (2007).
[7] X. J. Wang, F. Q. Wan, K. Han, C. X. Chai, K. Jiang, Mater Charact. **59**, 1765–70 (2008).
[8] F. Lu, W. P. Cai, Y. G. Zhang, Y. Li, F. Q. Sun, J Phys Chem C **111**, 13385-92 (2007).
[9] S. M. Reda, S. A. El-Sherbieny, J Mater Res. **25**, 522-8 (2010).
[10] J. X. Ding, J. A. Zapien, W. W. Chen, Y. Lifshitz, S. T. Lee, Appl Phys Lett. **85**, 2361-3 (2004).
[11] J. A. Zapien, Y. Jiang, X. M. Meng, W. Chen, Au FCK, Lifshitz Y, et al. Appl Phys Lett. **84**, 1189-91 (2004).
[12] X. Y. Wang, Y. C. Zhu, H. Fan, M. F. Zhang, B. J. Xi, H. Z. Wang, et al. J Cryst Growth; **310**, 2525–31 (2008).
[13] X. Jiang, Y. Xie, J. Lu, L. Zhu, W. He, Y. Qian, Chem Mater. **13**, 1213-18 (2001).
[14] Z. G. Chen, J. Zou, G. Liu, H. F. Lu, F. Li, G. Q. Lu, et al, Nanotechnology **19**, 055710 (2008).
[15] R. F. Zhuo, H. T. Feng, D. Yan, J. T. Chen, J. J. Feng, J. Z. Liu, et al. J Cryst Growth, **310**, 3240–6 (2008).
[16] M. Chang, X. L. Cao, X. J. Xu, L. D. Zhang, Phys Lett A **372**, 273–6 (2008).
[17] Q. H. Xiong, G. Chen, J. D. Acord, X. Liu, J. J. Zengel, H. R. Gutierrez, et al. Nano Lett; **4**, 1663–8 (2004).
[18] F. Fang, J. Kennedy, J. Futter, T. Hopf, A. Markwitz, E. Manikandan, et al. Nanotechnology **22**, 335702 (2011).
[19] S. Iijima, Nature; **354**, 56-8 (1991).
[20] Y. Q. Zhu, H. W. Kroto, D. R. M. Walton, H. Lange, A. Huczko, Chem Phys Lett. **365**, 457–63 (2002).
[21] Y. C. Choi, W. S. Kim, Y. S. Park, S. M. Lee, D. J. Bae, Y. H. Lee, et al. Adv Mater; **12**, 746-50 (2000).
[22] F. Fang, J. Futter, A. Markwitz, J. Kennedy, Nanotechnology, **20**, 245502 (2009).
[23] X. F. Wu, C. X. Xu, G. P. Zhu, Y. M. Ling, Chin Phys Lett. **23**, 2165-8 (2006).
[24] G. P. Zhu, C. X. Xu, X. F. Wu, Y. Yang, X. W. Sun, Y. P. Cui, J Electron Mater. **36**, 494-7 (2007).
[25] M. Wang, G. T. Fei, X. G. Zhu, B. Wu, M. G. Kong, L. D. Zhang, J Phys Chem C; **113**, 4335–9 (2009).
[26] D. P. Wei, Y. Ma, H. Y. Pan, Q. Chen, J Phys Chem C; **112**, 8594–9 (2008).
[27] P. D. Yang, C. M. Lieber, J Mater Res; **12**, 2981-96 (1997).
[28] W. G. Becker, A. J. Bard, J Phys Chem. **87**, 4888-93 (1983).
[29] Y. Yang, W. J. Zhang, Mater Lett. **58**, 3836–8 (2004).
[30] Y. W. Wang, L. D. Zhang, C. H. Liang, G. Z. Wang, X. S. Peng, Chem Phys Lett; **357**, 314–8 (2002).
[31] Y. Jiang, X. M. Meng, J. Liu, Z. Y. Xie, C. S. Lee, S. T. Lee, Adv Mater. **15**, 323-7 (2003).

*Corresponding author: wuxf@seu.edu.cn